Piroxicam; A novel corrosion inhibitor for mild steel corrosion in HCl acid solution

A. K. Singh, M. A. Quraishi*

Department of Applied Chemistry, Institute of Technology Banaras Hindu University, Varanasi 221 005 (India)

*Corresponding author: E-mail: maquraishi@rediffmail.com; maquraishi.apc@itbhu.ac.in
Tel. +91-9307025126; Fax: +91- 542- 2368428

Abstract

The corrosion inhibition properties of piroxicam (PRX) for mild steel corrosion in HCl solution were analysed by electrochemical impedance spectroscopy (EIS), potentiodynamic polarization and gravimetric methods. Physical adsorption is proposed for the inhibition and the process followed the Langmuir adsorption isotherm. The mechanism of adsorption inhibition and type of adsorption isotherm were proposed from the trend of inhibition efficiency with temperature, E_a and ΔG^o_{ads}. Potentiodynamic polarization study clearly revealed that piroxicam acted as mixed type inhibitor. The experimental data showed a frequency distribution and therefore a modelling element with frequency dispersion behaviour, a constant phase element (CPE) has been used.

Key Words: EIS; Acid solutions; Mild steel; potentiodynamic polarization; acid inhibition

1. Introduction

Mild steel is widely applied as the constructional material in many industries due to its excellent mechanical properties and low cost. The main problem of applying mild steel is its dissolution in acidic solutions. Recently, the inhibition of mild steel corrosion in acid solutions by different types of organic inhibitors has been extensively studied [1-4].

The use of inhibitors is the most economical and practical methods of reducing corrosive attack on metals [5-7]. During the past decade, the inhibition of mild steel corrosion in acid solutions by various types of organic inhibitors has attracted much attention [8, 9]. There is a continuing effort to find a corrosion inhibitor that exhibits a greater effect with a smaller quantity in the corrosion medium. This is a challenging problem in the steel industry because corrosion over mild steel surfaces affects long term industrial projects. The performance of the corrosion inhibitors based on organic compounds containing nitrogen, sulphur and oxygen atoms shows promising results. The inhibitors influence the kinetics of the electrochemical reactions which constitute the corrosion process and thereby modify the metal dissolution in acids. The existing data show that most organic inhibitors act by adsorption on the metal surface. They change the structure of the electrical double layer by adsorption on the metal surface

This article reported our attempt to use electrochemical impedance spectroscopy (EIS), potentiodynamic polarization and weight loss method to investigate the nature of adsorption of piroxicam on the mild steel surface. The structure of piroxicam is shown in Figure 1.
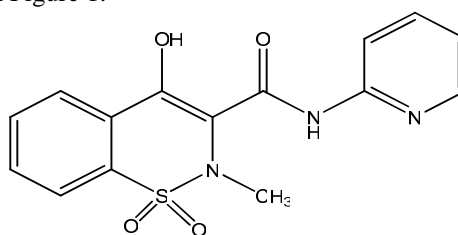

Figure 1 Structure of Piroxicam molecule

2. Experimental

2.1 Inhibitor
The studied compound piroxicam, a non-steroidal anti-inflammatory drug, is available under the brand name feldene. Stock solution of piroxicam was made in 10:1 ratio water: ethanol mixture to ensure solubility. This stock solution was used for all experimental purposes.

2.2 Corrosion measurements
Prior to all measurements, the mild steel specimens, having composition (wt %) C = 0.17, Mn= 0.46, Si = 0.26, S = 0.017, P = 0.019 and balance Fe, were abraded successively with emery papers from 600 to 1200 grade. The specimen were washed thoroughly with double distilled water, degreased with acetone and finally dried in hot air blower. After drying, the specimen were placed in desiccator and then used for experiment. The aggressive solution 1 M HCl was prepared by dilution of analytical grade HCl with double distilled water and all experiments were carried out in unstirred solutions. The rectangular specimens with dimension $2.5 \times 2.0 \times 0.025$ cm were used in weight loss experiments and of size 1.0 cm $\times$ 1.0 cm (exposed) with a 7.5 cm long stem (isolated with commercially available lacquer) were used for electrochemical measurements.

2.3 Electrochemical impedance spectroscopy
The EIS tests were performed at 303 ±1 K in a three electrode assembly. A saturated calomel electrode was used as the reference; a 1 cm^2 platinum foil was used as counter electrode. All potentials are reported vs. SCE. Electrochemical impedance spectroscopy measurements (EIS) were performed using a Gamry instrument Potentiostat/Galvanostat with a Gamry framework system based on ESA 400 in a frequency range of 100000 Hz to 0.01 Hz under potentiodynamic conditions, with amplitude of 10 mV peak-to-peak, using AC signal at E_{corr}. Gamry applications include software DC105 for corrosion and EIS300 for EIS measurements, and Echem Analyst version 5.50 software packages for data fitting. The experiments were measured after 30 min. of immersion in the testing solution (no deaeration, no stirring). The working electrode was prepared from a square sheet of mild steel such that the area exposed to solution was 1 cm^2.

The charge transfer resistance values were obtained from the diameter of the semi circles of the Nyquist plots. The inhibition efficiency of the inhibitor was calculated from the charge transfer resistance values using the following Eqn.

$$E\% = \frac{R_{ct}^{i} - R_{ct}^{0}}{R_{ct}^{i}} \times 100 \tag{1}$$

where R_{ct}^{0} and R_{ct}^{i} are the charge transfer resistance in absence and in presence of inhibitor, respectively.

2.4 Potentiodynamic polarization
The electrochemical behaviour of mild steel sample in inhibited and non-inhibited solution was studied by recording anodic and cathodic potentiodynamic polarization curves. Measurements were performed in the 1 M HCl solution containing different concentrations of the tested inhibitors by changing the electrode potential automatically from -250 to +250 mV vs. corrosion potential at a scan rate of 1 mV s^{-1}. The linear Tafel segments of anodic and cathodic curves were extrapolated to corrosion potential to obtain corrosion current densities (I_{corr}).

The inhibition efficiency was evaluated from the measured I_{corr} values using the relationship:

$$E\% = \frac{I_{corr}^{0} - I_{corr}^{i}}{I_{corr}^{0}} \times 100 \tag{2}$$

where, I_{corr}^{0} and I_{corr}^{i} are the corrosion current density in absence and presence of inhibitor, respectively.

2.5 Linear polarization measurement
The corrosion behaviour was studied with polarization resistance measurements (R_p) in 1 M HCl solution with and without different concentrations of studied inhibitors. The linear polarization study was carried out from cathodic potential of -20 mV vs. OCP to an anodic potential of + 20 mV vs. OCP at a scan rate 0.125 mV s^{-1} to study the polarization resistance (R_p) and the polarization resistance was evaluated from the slope of curve in the vicinity of corrosion potential. From the evaluated polarization resistance value, the inhibition efficiency was calculated using the relationship:

$$E\% = \frac{R_{p}^{i} - R_{p}^{0}}{R_{p}^{i}} \times 100 \tag{3}$$

where, R_{p}^{0} and R_{p}^{i} are the polarization resistance in absence and presence of inhibitor, respectively.

2.6 Weight loss measurements

Weight loss measurements were performed on rectangular mild steel samples having size $2.5 \times 2.0 \times 0.025$ cm by immersing the mild steel coupons into acid solution (100 mL) without and with different concentrations of isoniazid derivatives. After the elapsed time, the specimen were taken out, washed, dried and weighed accurately. All the tests were conducted in aerated 1 M HCl. All the experiments were performed in triplicate and average values were reported. From the evaluated weight loss, the surface coverage (θ) and inhibition efficiency ($E\%$) was calculated using:

$$\theta = \frac{w_0 - w_i}{w_0} \tag{4}$$

$$E\% = \frac{w_0 - w_i}{w_0} \tag{5}$$

where, θ is surface coverage, w_0 is weight loss in free acid solution and w_i is weight loss in acid solution in presence of inhibitor, respectively.

3. Results and Discussion

3.1Electrochemical impedance spectroscopy

The corrosion behaviour of mild steel in 1 M HCl in absence and presence of piroxicam were investigated by EIS after immersion for 30 min at 303 ± 1 K. Nyquist plots of mild steel in uninhibited and inhibited acid solutions containing 200 ppm concentrations of piroxicam are presented in Figure 2a. EIS spectra obtained consists of one depressed capacitive loop (one time constant in Bode-phase plot). The increased diameter of capacitive loop obtained in 1 M HCl in presence of piroxicam indicated the inhibition of corrosion of mild steel. The high frequency capacitive loop may be attributed to the charge transfer reaction.
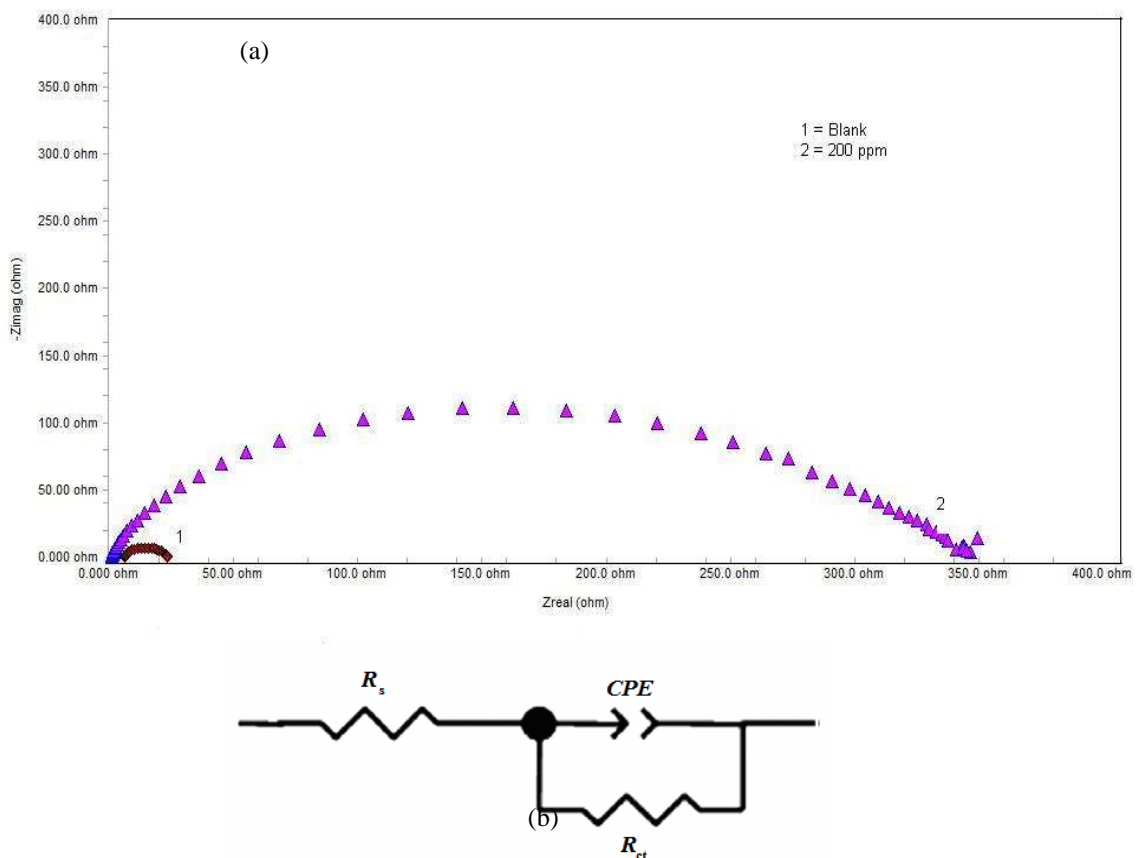

Figure 2   (a) Nyquist plots in absence and presence of 200 ppm concentration of piroxicam and (b) The electrochemical equivalent circuit used to fit the impedance measurements that include a solution resistance (R_s), a constant phase element (*CPE*) and a polarization resistance or charge transfer (R_{ct})

Corrosion kinetic parameters derived from EIS measurements and inhibition efficiencies are given in Table 1. Double layer capacitance (C_{dl}) and charge transfer resistance (R_{ct}) were obtained from EIS measurements as described elsewhere [10]. It is apparent from Table 1 that the impedance of the inhibited system amplified with the inhibitor the C_{dl} values decreased with inhibitor. This decrease in C_{dl} results from a decrease in local dielectric constant and/or an increase in the thickness of the double layer, suggested that inhibitor molecules inhibit the iron corrosion by adsorption at the metal/acid interface [11]. The depression in Nyquist semicircles is a feature for solid electrodes and often referred to as frequency dispersion and attributed to the roughness and other inhomogenities of the solid electrode [12]. In this behaviour of solid electrodes, the parallel network: charge transfer resistance-double layer capacitance is established where an inhibitor is present. For the description of a frequency independent phase shift between an applied ac potential and its current response, a constant phase element (CPE) is used which is defined in impedance representation as in Eqn. (6)

$$Z_{CPE} = Y_0^{-1}(i\omega)^{-n} \tag{6}$$

where, Y_0 is the CPE constant, ω is the angular frequency (in rad s^{-1}), $i^2 = -1$ is the imaginary number and n is a CPE exponent which can be used as a gauge of the heterogeneity or roughness of the surface [13]. Depending on the value of n, CPE can represent resistance (n = 0, Y_0 = R), capacitance (n = 1, Y_0 = C), inductance (n = -1, Y_0 = L) or Warburg impedance (n = 0.5, Y_0 = W).

Figure 2b showed the electrical equivalent circuit employed to analyse the impedance spectra. Excellent fit with this model was obtained for all experimental data.

The electrochemical parameters, including R_s, R_{ct}, Y_0 and n, obtained from fitting the recorded EIS data using the electrochemical circuit of Figure 3 are listed in Table 1. C_{dl} values derived from CPE parameters according to Eqn. (7) are listed in Table 1:

$$C_{dl} = (Y_0 . R_{ct}^{1-n})^{1/n} \tag{7}$$

Table 1. Impedance parameters and inhibition efficiency values for mild steel after 30 min immersion period in 1 M HCl in absence and presence of 200 ppm of piroxicam

Inhibitor	Conc. (ppm)	R_s (Ω cm^2)	R_{ct} (Ω cm^2)	C_{dl} (μF cm^{-2})	E%
Piroxicam	-	1.07	11	66	-
	200	0.82	324	37	97

3.2 Potentiodynamic polarization measurements

Polarization measurements were carried out in order to gain knowledge concerning the kinetics of the cathodic and anodic reactions. Figure 3 presented the results of the effect of piroxicam on the cathodic and anodic polarization curves of mild steel in 1 M HCl, respectively. It could be observed that both the cathodic and anodic reactions were suppressed with the addition of piroxicam, which suggested that the piroxicam reduced anodic dissolution and also retarded the hydrogen evolution reaction. Electrochemical corrosion kinetics parameters, i.e. corrosion potential (E_{corr}), cathodic and anodic Tafel slopes (b_a, b_c) and corrosion current density (I_{corr}) obtained from the extrapolation of the polarization curves, were given in Table 2.

Table 2. Potentiodynamic polarization parameters for mild steel in absence and presence of 200 ppm piroxicam in 1 M HCl

Inhibitor	Conc. (ppm)	Tafel data					Linear polarization data	
		E_{corr} (mV vs. SCE)	I_{corr} (μA cm^{-2})	b_a (mV dec^{-1})	b_c (mV dec^{-1})	E%	R_p (Ω cm^2)	E%
Piroxicam	-	-471	1050	95	173	-	17.2	-
	200	-468	84	96	182	92	324	97

The parallel cathodic Tafel curves in Figure 3 suggested that the hydrogen evolution is activation-controlled and the reduction mechanism is not affected by the presence of the inhibitor. The region between linear part of cathodic and anodic branch of polarization curves becomes wider as the inhibitor is added to the acid solution. Similar results were found in the literature [14]. The values of b_c changed with increasing inhibitor concentration, indicated the influence of the compounds on the kinetics of hydrogen evolution.

Due to the presence of some active sites, such as aromatic rings, hetero-atoms in the studied compound for making adsorption, they may act as adsorption inhibitors. Being absorbed on the metal surface, these compounds controlled the anodic and cathodic reactions during corrosion process, and then their corrosion

inhibition efficiencies are directly proportional to the amount of adsorbed inhibitor. The functional groups and structure of the inhibitor play important roles during the adsorption process. On the other hand, an electron transfer takes place during adsorption of the neutral organic compounds at metal surface [15]. As it can be seen from Table 2, the studied inhibitor reduced both anodic and cathodic currents with a slight shift in corrosion potential (3 mV). According to Ferreira and others [16, 17], if the displacement in corrosion potential is more than 85mV with respect to corrosion potential of the blank solution, the inhibitor can be seen as a cathodic or anodic type. In the present study, the displacement was 3 mV which indicated that the studied inhibitor is mixed-type inhibitor. The results obtained from Tafel polarization showed good agreement with the results obtained from EIS.
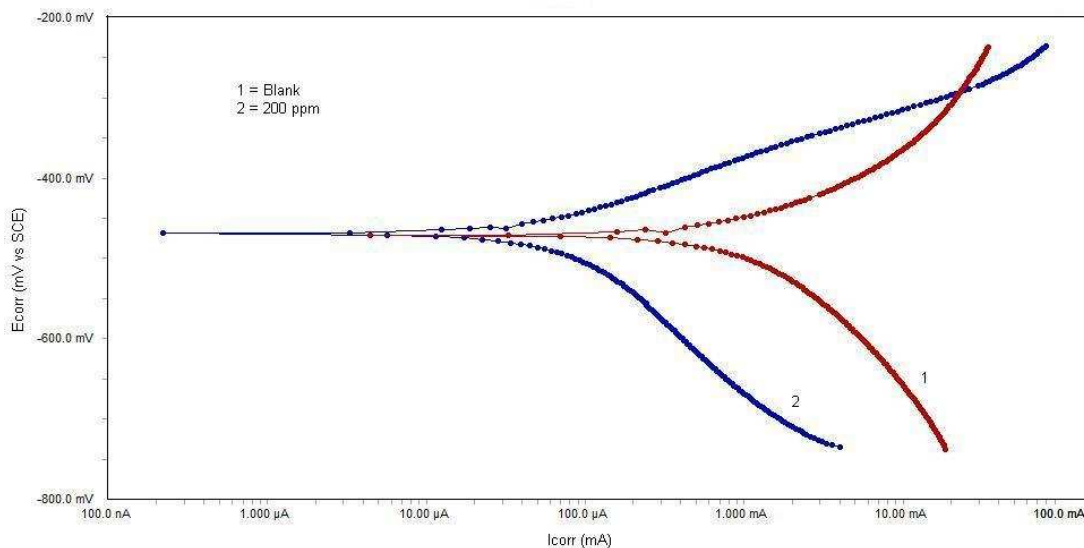

Figure 3   Typical polarization curves for corrosion of mild steel in 1 M HCl in the absence and presence of 200 ppm concentration of piroxicam

3.3. Linear polarization resistance
Polarization resistance values were determined from the slope of the potential–current lines,

$$R_p = A\frac{dE}{dI} \tag{8}$$

where *A* is surface area of electrode, d*E* is change in potential and d*I* is change in current. The inhibition efficiencies and polarization resistance parameters are presented in Table 2. The results obtained from Tafel polarization and EIS showed good agreement with the results obtained from linear polarization resistance.
3.6 Weight loss measurement

3.6.1 Effect of inhibitor concentration
Figure 4a showed the trend of inhibition efficiencies obtained from weight loss measurements for different concentrations of piroxicam in 1 M HCl after 3 h immersion at 308 K. It followed from the Figure 9a that the inhibition efficiency increased with increase in inhibitor concentration. This trend may result from the fact that adsorption and surface coverage increased with the increase in piroxicam concentration.

3.6.2 Effect of immersion time
The effect of increasing time on the efficiency of piroxicam is shown in Figure 4b. At 200 ppm, increasing immersion time resulted in increase in efficiency upto 4 h but thereafter decrease in inhibition efficiency. The decrease in inhibition efficiency can be attributed to desorption of inhibitor from mild steel surface.

3.6.4 Effect of temperature
The effect of temperature on the performance of the inhibitor at a concentration of 200 ppm for mild steel in 1 M HCl at 308, 318, 328 and 338 K was studied using weight loss measurements as shown in Figure 4c. The corrosion rate increased with increasing temperature both in free and inhibited acid. It could be seen that piroxicam had good inhibition efficiency ($E\%$) against corrosion of mild steel in HCl solution, but, decreased with increasing temperature, which suggested that corrosion inhibition of mild steel by piroxicam caused by the adsorption of inhibitor molecule while higher temperatures caused the desorption of piroxicam from the mild steel surface [5].
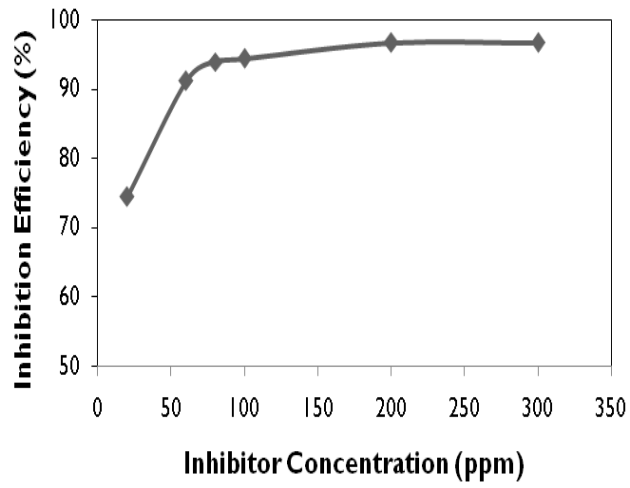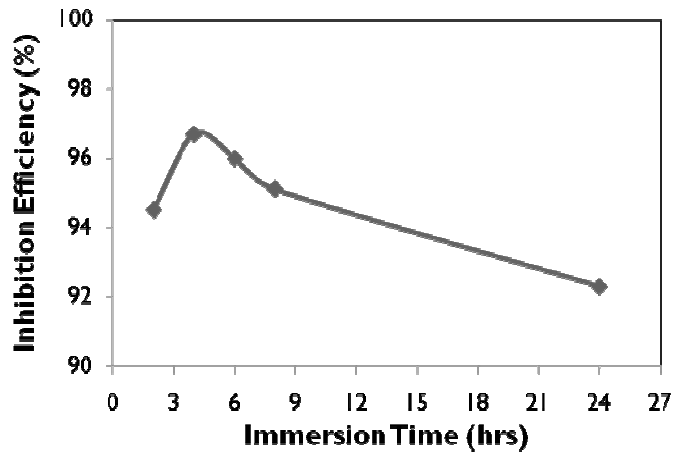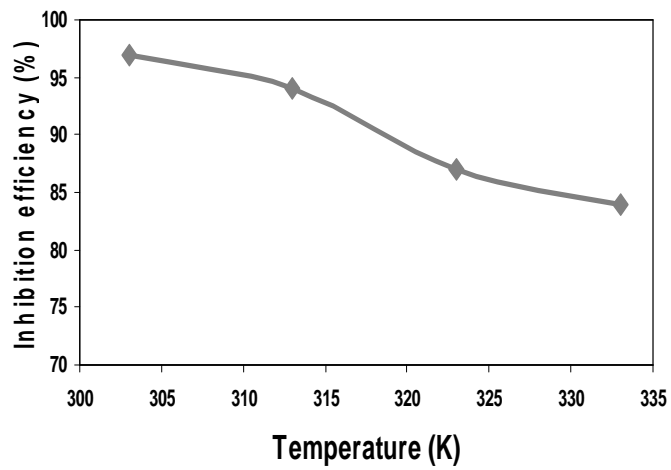
Figure 4a

Figure 4b

Figure 4c

Figure 4 Variation of inhibition efficiency with (a) concentration of inhibitor, (b) immersion time and (c) temperature of the solution

106

3.7 Adsorption isotherm

Adsorption depends mainly on the charge and nature of the metal surface, electronic characteristics of the metal surface, adsorption of solvent and other ionic species, temperature of corrosion reaction and on the electrochemical potential at solution-interface. Adsorption of inhibitor involves the formation of two types of interaction responsible for bonding of inhibitor to a metal surface. The first one (physical adsorption) is weak undirected interaction and is due to electrostatic attraction between inhibiting organic ions or dipoles and the electrically charged surface of metal. The potential of zero charge plays an important role in the electrostatic adsorption process. The charge on metal surface can be expressed in terms of potential difference ($\square$) between the corrosion potential (E_{corr}) and the potential of zero charge (E_{pzc}) of the metal ($\phi = E_{corr} - E_{pzc}$). If $\square$ is negative, adsorption of cations is favoured. On the contrary, the adsorption of anions is favourable if $\square$ is positive. The second type of interaction (adsorption) occurs when directed forces govern the interaction between the adsorbate and adsorbent. Chemical adsorption involves charge sharing or charge transfer from adsorbates to the metal surface atoms in order to form a coordinate type of bond. Chemical adsorption has a free energy of adsorption and activation energy higher than physical adsorption and, hence, usually it is irreversible [18]. Adsorption isotherms are usually used to describe the adsorption process. The establishment of adsorption isotherms that describe the adsorption of a corrosion inhibitor can provide important clues to the nature of the metal- inhibitor interaction. Adsorption of the organic molecules occurs as the interaction energy between molecule and metal surface is higher than that between the H_2O molecule and the metal surface [19].

In order to obtain the adsorption isotherm, the degree of surface coverage (θ) for various concentrations of the inhibitor has been calculated according to Eqn. (4). Langmuir isotherm was tested for its fit to the experimental data. Langmuir isotherm is given by following equation:

$$\frac{C_{inh}}{\theta} = \frac{1}{K_{ads}} + C_{inh} \tag{9}$$

where K_{ads} is the equilibrium constant of the adsorption-desorption process, θ is the degree of surface coverage and C_{inh} is concentration of inhibitor in the bulk solution. Langmuir isotherm was found best fit for the adsorption of piroxicam on the mild steel surface in HCl solution (Figure 5)
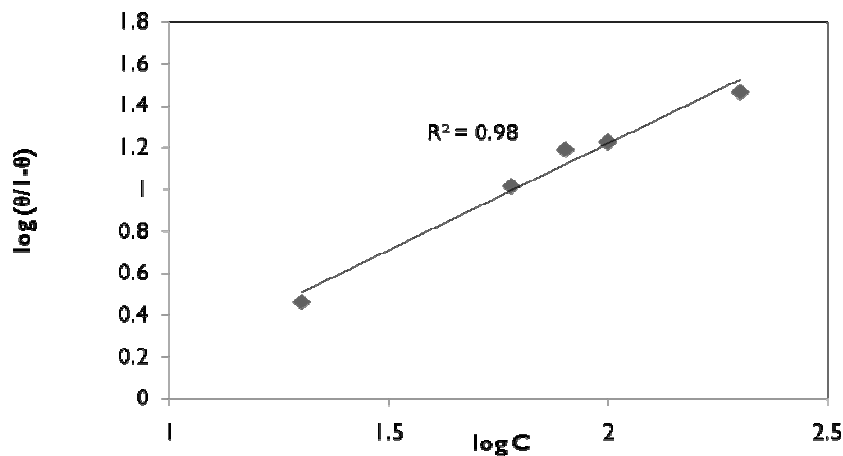

Figure 5 Langmuir adsorption isotherm for the adsorption of piroxicam on the mild steel surface in 1 M HCl

3.8 Kinetic and thermodynamic considerations

The dependence of corrosion rate at temperature can be expressed by Arrhenius equation and transition state Eqn. [20-22]:

$$\log(CR) = \frac{-E_a}{2.303RT} + \log \lambda \tag{10}$$

$$CR = \frac{RT}{Nh} \exp\left(\frac{\Delta S^*}{R}\right) \exp\left(-\frac{\Delta H^*}{RT}\right) \tag{11}$$

where E_a apparent activation energy, λ the pre-exponential factor, ΔH^* the apparent enthalpy of activation, ΔS^* the apparent entropy of activation, h Planck's constant and N the Avogadro number, respectively. The apparent activation energy and pre-exponential factors in absence and presence of 200 ppm concentration of

piroxicam can be calculated by linear regression between $\log CR$ and $1/T$, the results were shown in Table 3. Figure 6a depicted an Arrhenius plots for mild steel immersed in 1 M HCl in absence and presence of 200 ppm concentration of piroxicam. The plots obtained are straight lines and the slope of each straight line gives its apparent activation energy. Table 3 presented E_a and λ values in absence and presence of 200 ppm concentration of piroxicam. Inspection of Table 3 showed that apparent activation energy increased with inhibitor.
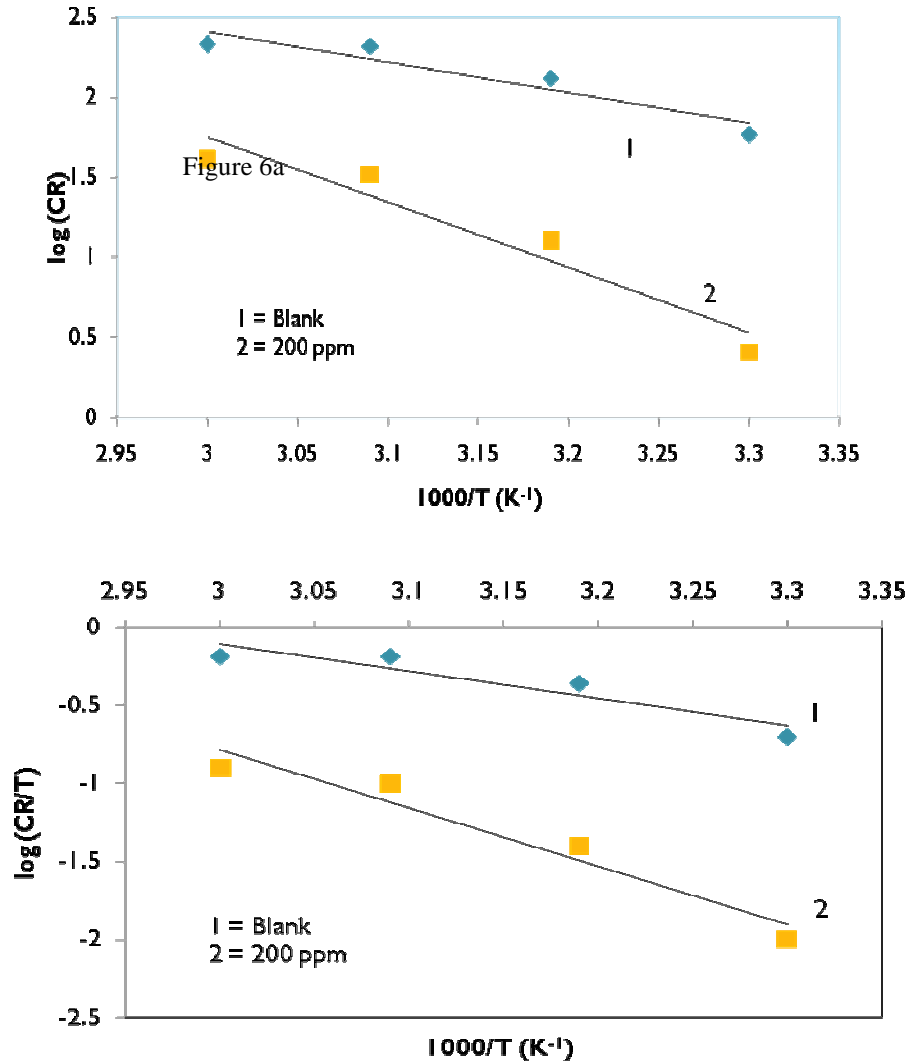

Figure 6 Adsorption isotherm plots in absence and presence of 200 ppm concentration of piroxicam for (a) log C_R vs. $1/T$ and (b) log (C_R/T) vs. $1/T$

The increase in E_a could be interpreted as the physical adsorption. Szauer and Brand [23] explained that the increase in activation energy can be attributed to an appreciable decrease in the adsorption of the inhibitor on the mild steel surface with increase in temperature and a corresponding increase in corrosion rates occurs due to the fact that greater area of metal is exposed to the acid environment.

Table 3. Thermodynamic activation parameters for mild steel in 1 M HCl in absence and presence of 200 ppm piroxicam

Inhibitor conc. (ppm)	E_a (kJ mol^{-1})	ΔH^* (kJ mol^{-1})	ΔS^* (J K^{-1} mol^{-1})
-	37	33	-100
200	78	72	3

According to Eqn. (11), corrosion rate (*CR*) is being affected by both E_a and λ. In general, the influence of E_a on the mild steel corrosion is higher than that of λ. However, if the variation in λ was drastically higher than that of λ, the value of λ might be the dominant factor to determine the mild steel corrosion. In present case, E_a and λ increased with inhibitor (the higher E_a and lower λ led to lower corrosion rate). As it can be seen from Figure 6a, the corrosion rate of steel decreased with inhibitor; hence, it is clear that increment of E_a is the decisive factor affecting the corrosion rate of mild steel in 1 M HCl.

The relationship between $\log(CR/T)$ and $1/T$ were shown in Figure 6b. Straight lines are obtained with a slope ($-\Delta H^*/2.303R$) and an intercept of $\left[\log(R/Nh)+(\Delta S^*/2.303R)\right]$, from which the value of ΔH^* and ΔS^* were calculated and presented in Table 3. The positive sign of enthalpy reflect the endothermic nature of steel dissolution process meaning that dissolution of steel is difficult. On comparing the values of entropy of activation (ΔS^*) listed in Table 3, it is clear that entropy of activation increased in presence of the studied inhibitor compared to free acid solution. Such variation is associated with the phenomenon of ordering and disordering of inhibitor molecules on the mild steel surface. The increased entropy of activation in the presence of inhibitors indicated that disorderness is increased on going from reactant to activated complex.

The equilibrium constant for the adsorption process from Langmuir isotherm is related to the standard free energy of adsorption by the expression:

$$K_{ads} = \frac{1}{55.5}\exp\left[\frac{-\Delta G^o_{ads}}{RT}\right] \tag{12}$$

where, R is the molar gas constant, T is the absolute temperature and 55.5 is the concentration of water in solution expressed in molar. The standard free energy of adsorption, ΔG^o_{ads}, which can characterize the interaction of adsorption molecules and metal surface, was calculated by equation (13). The negative values of ΔG^o_{ads} ensure the spontaneity of adsorption process and stability of the adsorbed layer on the mild steel surface. Generally, the values of around -20kJ mol^{-1} or lower are consistent with physisorption, while those around -40 kJ mol^{-1} or higher involve chemisorptions [24]. The values of ΔG^o_{ads} for piroxicam are given in Table 4 and these values indicate that piroxicam molecules are physisorbed onto mild steel surface. The adsorption is enhanced by the presence of three N atoms with lone pairs of electrons and the delocalized π-electrons in the inhibitor molecules that makes it adsorbed electrostatically on the metal surface forming insoluble stable films on the metal surface thus decreasing metal dissolution.

Table 4. Thermodynamic parameters for the adsorption of piroxicam in 1 M HCl on the mild steel at different temperatures

Inhibitor conc. (ppm)	Temperature (K)	K_{ads} (10^4 M^{-1})	ΔG^o_{ads} (kJ mol^{-1})
200	303	10.9	-17.1
	313	4.8	-16.7
	323	2.6	-16.5
	333	2.0	-16.3

4. Mechanism of inhibition

The inhibition efficiency of piroxicam against the corrosion of mild steel in 1 M HCl can be explained on the basis of the number of adsorption sites, molecular size and mode of interaction with the metal surface [25, 26]. Physical adsorption requires presence of both electrically charged surface of the metal and charged species in the bulk of the solution; the presence of a metal having vacant low-energy electron orbital and of an inhibitor with molecules having relatively loosely bound electrons or heteroatoms with lone pair electrons. However, the compound reported is an organic base which can be protonated in an acid medium. Thus they become cations, existing in equilibrium with the corresponding molecular form

$$PRX \quad + \quad x\text{H}^+ \quad \leftrightarrow \quad \left[PRX_x\right]^{x+} \tag{13}$$
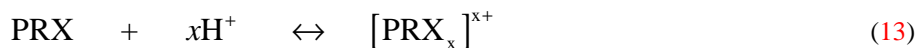
The protonated piroxicam, however, could be attached to the mild steel surface by means of electrostatic interaction between Cl$^-$ and protonated piroxicam since the mild steel surface has positive charge in the HCl

medium [5]. This could further be explained based on the assumption that in the presence of Cl^-, the negatively charged Cl^- would attach to positively charged surface. When piroxicam adsorbs on the mild steel surface, electrostatic interaction takes place by partial transference of electrons from the polar atom (N atom and delocalized π-electrons of the aromatic ring) of piroxicam to the metal surface.

5. Conclusion

The following main conclusions are drawn from the present study:
1. Piroxicam was found to be a good inhibitor for mild steel corrosion in acid medium.
2. The inhibition efficiency of piroxicam decreased with temperature, which leads to an increase in activation energy of the corrosion process.
3. Potentiodynamic polarization curves revealed that piroxicam is a mixed-type inhibitor

Acknowledgement

References

1. Singh, A.K., Quraishi, M.A. *Mater. Chem. Phys.* 123 (2010) 666.
2. Singh, A.K., Quraishi, M.A. *J. Appl. Electrochem.* 40 (2010) 1293.
3. El Sherbini, E.E. *F. Mater. Chem. Phys.* 61 (1999) 223.
4. Morad, M.S. *Corros. Sci.* 50 (2008) 436.
5. Singh, A.K. Quraishi, M.A. *Corros. Sci.* 51 (2009) 2752.
6. Singh, A.K. Quraishi, M.A. *Corros. Sci.* 52 (2010) 152.
7. Singh, A.K. Quraishi, M.A. *Corros. Sci.* 52 (2010)1529.
8. Asan, A. Soylu, S. Kıyak, T. Yıldırım, F. Oztas, S. G. Ancın, N. Kabasakaloglu, M. *Corros. Sci.* 48 (2006) 3933.
9. Lebrini, M. Bentiss, F. Vezin, H. Lagrenee, M. *Corros. Sci.* (2006) 1279.
10 Singh, A.K. Quraishi, M.A. *Corros. Sci.* 52 (2010) 1373.
11. Bentiss, F. Jama, C. Mernari, B. Attari, H.E. Kadi, L. E. Lebrini, M. Traisnel, M. Lagrenee, M. *Corros. Sci.* 51 (2009)1628.
12. Ashassi-Sorkhabi, H. Seifzadeh, D. Hosseini, M. G. *Corros. Sci.* 50 (2008) 3363.
13. Popova, A. Christov, M. *Corros. Sci.* 48 (2006) 3208.
14. Morad, M.S. Kamal El-Dean, A. M. *Corros. Sci.* 48 (2006) 3398.
15. Ozcan, M. Dehri, I. Erbil, M. *Appl. Surf. Sci.* 236 (2004) 155.
16. Ferreira, E.S. Giancomelli, C. Giacomelli, F. C. Spinelli, A. *Mater. Chem. Phys.* 83 (2004) 129.
17. Li, W.H. He, Q. Pei, C. L. Hou, B. R. *J. Appl. Electrochem.* 38 (2008) 289.
18. Trabanelli, G., in: Mansfeld F (Ed.), *Corrosion mechanism,* Mercel Dekker, New York, 1987
19. McCafferty, E.in: Leidheiser Jr. H (Ed.), *Corrosion control by coating*, Science Press, Princeton, 1979.
20. Li, X. Tang, L. *Mater. Chem. Phys.* 90 (2005) 286.
21. Noor, E.A. Al-Moubaraki, A.H. *Mater. Chem. Phys.* 110 (2008) 145.
22. Umoren, S.A. Ogbobe, O. Igwe, I.O. Ebenso, E.E. *Corros. Sci.* 50 (2008) 1998.
23. Szauer, T. Brandt, A. *Electrochim. Acta* 26 (1981) 245.
24. Umoren, S.A. Obot, I.B. Ebenso, E.E. Okafor, P.C. Ogbobe, O. Oguzie, E.E. *Anti-Corros. Method Mater*. 53 (2006) 277.
25. Fouda, A.S., Moussa, M., Taha, F. El-Neanae, A. *Corros. Sci*. 26 (1986) 719.
26. Singh, A.K., Quraishi, M.A. *J. Appl. Electrochem.* 40 (2010) 1293.

(2010) www.jmaterenvironsci.com